Identification and Localization of a Novel, Cytoskeletal, Centrosome-associated Protein in PtK2 Cells

Andre T. Baron and Jeffrey L. Salisbury

Laboratory for Cell Biology, Center for NeuroSciences, Case Western Reserve University, School of Medicine, Cleveland, Ohio 44106

Abstract. Antisera raised against centrin (Salisbury, J. L., A. T. Baron, B. Surek, and M. Melkonian. 1984. *J. Cell Biol.* 99:962–970) have been used, here, to identify a centrosome-associated protein with an M_r of 165,000. Immunocytochemistry indicates that this protein is a component of pericentriolar satellites, basal feet, and pericentriolar matrix of interphase cells. These components of pericentriolar material are, in part, composed of 3–8-nm-diam filaments, which interconnect to form a three-dimensional pericentriolar lattice. We conclude that the 165,000-M_r protein is immunologically related to centrin, and that it is a component of a novel centrosome-associated cytoskeletal filament system.

Microtubule organizing centers such as the flagellar apparatus of algal cells, spindle pole body of yeast cells, and centrosome of mammalian cells are homologous structures essential for cytoplasmic organization and cellular proliferation. Molecular cloning studies have recently shown that the cell cycle gene product CDC31, required for spindle pole body duplication, shares 50% sequence homology with centrin (Huang, B., A. Mengersen, and V. D. Lee. 1988. *J. Cell Biol.* 107:133–140). The evolutionary conservation of centrin-related sequences and immunologic epitopes to microtubule organizing centers of divergent phylogeny suggests that a functional attribute(s) may have been conserved as well. Elucidation of a common thread between these related molecules may be fundamental to our understanding of cell structure and function.

THE centrosome and mitotic spindle poles are the major microtubule organizing centers (MTOCs)[1] (Pickett-Heaps, 1969) of interphase and mitotic animal cells, respectively (Brinkley, 1985; Karsenti and Maro, 1986). The functional integrity of these MTOCs is essential for the determination of cell shape and polarity (McIntosh, 1983), and for motility phenomena such as directed cell migration (Albrecht-Buehler, 1977; Gotlieb et al., 1981; Nemere et al., 1985) and cell division (McIntosh, 1987; Mazia, 1987). Depending on the phase of the cell cycle, the centrosome is characterized by the presence of two or four centrioles; each centriole pair is referred to as a diplosome or duplex. In addition to centrioles, the centrosome is defined by a convergent microtubule array, a variety of electron-opaque structures known as pericentriolar material (PCM), and smooth membrane tubules and vesicles (DeHarven, 1968; Brinkley and Stubblefield, 1970; Wolfe, 1972; Peterson and Berns, 1980; Brinkley, 1985; Karsenti and Maro, 1986).

Included under the category of PCM are the following structures: a fibrillar halo or cloud of osmophilic electron-opaque material that surrounds the centrioles (pericentriolar matrix); compact electron-opaque bodies known as pericentriolar satellites; and a variety of centriolar "appendages." The role of PCM, not the centrioles, as the preferential site for nucleating and anchoring cytoplasmic microtubules has become well established (Tilney and Goddard, 1970; Berns et al., 1977; Berns and Richardson, 1977; Gould and Borisy, 1977; Telzer and Rosenbaum, 1979; Kuriyama and Borisy, 1981a; Rieder and Borisy, 1981). In spite of the importance of PCM in MTOC function, a precise structural characterization of (*a*) the various components of PCM, (*b*) its biochemical composition, and (*c*) its relationship to MTOC function have not been established.

In a previous report (Salisbury et al., 1984), we isolated and partially characterized striated flagellar roots (SFRs) from the alga *Tetraselmis striata*. These organelles integrate the basal bodies of the flagellar apparatus into the cytoplasm and are predominantly composed of an acidic 20,000-M_r calcium-binding protein, which has a phosphorylated isoform. We call this protein centrin. Antisera raised against centrin have been used to screen a variety of animal and algal cells by immunofluorescence microscopy (Salisbury et al., 1986; Schulze et al., 1987). For all cells examined, the antigenic determinant(s) was localized to the flagellar apparatus or centrosome. The flagellar apparatus is the major MTOC

---

1. *Abbreviations used in this paper:* MTOC, microtubule organizing center; PCM, pericentriolar material; PWB, Pipes wash buffer; SFR, striated flagellar root.

of algal cells (Ringo, 1967; Johnson and Porter, 1968; Coss, 1974; Doonan and Grief, 1987), and is functionally homologous to the centrosome of animal cells. The conservation of immunologic epitopes between such divergent MTOCs poses the possibility that some structural and functional attributes of centrin may also have been evolutionarily conserved.

In this study, we describe the fine structure of the mammalian centrosome with respect to striated roots, basal feet, and pericentriolar satellites—constituents of PCM. We identify a novel component of the centrosome that is immunologically related to centrin—a protein with an M_r of 165,000. Finally, using fluorescent and gold immunocytochemistry, we determine that this molecule is a component of basal feet, pericentriolar satellites, and pericentriolar matrix of interphase PtK$_2$ cells.

Materials and Methods

Cell Culture

PtK$_2$ cells were obtained from the American Type Culture Collection (Rockville, MD). They were grown on sterile glass coverslips in RPMI-1640 medium at 37°C and 5% CO$_2$ in air. The RPMI-1640 was supplemented with 10% FBS and penicillin-streptomycin, and buffered with 20 mM Hepes at pH 7.3. All culture reagents were purchased from Gibco Laboratories (Grand Island, NY).

Antibody Characterization

Antisera raised against centrin have been characterized in detail elsewhere (Salisbury et al., 1984).

In Vivo Labeling and Immunoprecipitation

Cell Culture. PtK$_2$ cells were subcultured 12 h before an experiment in 35-mm petri dishes to achieve an actively dividing population of cells at 80-90% confluence on the day of the experiment. The cells were grown as described above.

Preincubation and Labeling. To deplete the cells of methionine and cysteine they were washed with PBS (10 mM KH$_2$PO$_4$ and K$_2$HPO$_4$, 150 mM NaCl, pH 7.2), and preincubated in preincubation medium (DME minus methionine and cysteine, 5% dialyzed FBS, and L-glutamine) for 1 h at 37°C and 5% CO$_2$ in air. The cells were removed from preincubation medium and incubated in labeling medium (preincubation medium supplemented with [^{35}S]methionine and [^{35}S]cysteine [150 μCi/ml each]; Amersham Corp., Arlington Heights, IL) for 2 h at 37°C and 5% CO$_2$ in air.

Harvesting and Immunoprecipitation. Cells were washed with PBS, scraped from the petri dishes in PBS with a rubber policeman, transferred to microfuge tubes, and centrifuged (15,000 g; 5 s). The supernates were discarded and the cell pellets resuspended in 0.1 ml prewarmed (100°C) lysis buffer (0.5% NP-40, 0.5% deoxycholic acid, 2.5% SDS). After vortexing vigourously, 9 vol of immunoprecipitation buffer A (50 mM Tris-HCl, 190 mM NaCl, 6 mM EDTA, 2.5% Triton X-100, 100 U/ml trasylol, pH 7.4) were added to each cell lysate. After centrifugation (1-2 min), the postnuclear supernates were transferred to fresh microfuge tubes and incubated with the appropriate antibodies (anticentrin immune serum, preimmune serum, or no antiserum; ~15 μg/ml of Ig were used per sample) at 0-4°C overnight on a tumbler. Postnuclear supernates were incubated in 20 μl of packed protein A-Sepharose (Pharmacia Fine Chemicals, Inc., Uppsala, Sweden) in immunoprecipitation buffer B (10 mM Tris-HCl, 150 mM NaCl, 5 mM EDTA, 0.1% Triton X-100, 100 U/ml trasylol, pH 8.3) for an additional hour at 0-4°C on a tumbler. Protein A-Sepharose was pelleted by centrifugation (30 s) and washed with three changes of immunoprecipitation buffer B followed by TBS (10 mM Tris-HCl, pH 7.4, 150 mM NaCl). The final protein A-Sepharose pellets were loaded on a gel and run as described under Electrophoresis and Autoradiograpy.

Electrophoresis and Autoradiography

SDS-PAGE was carried out according to the method of Laemmli (1970) in slab gels containing 0.2% SDS and a 5-15% gradient of acrylamide. Gels were soaked in EN^{3}HANCE (New England Nuclear, Boston, MA) for 1 h, precipitated with running water, soaked in 5% glycerin for 15 min, dried, and recorded with Kodak XAR film (Eastman Kodak Co., Rochester, NY) at −70°C.

Immunofluorescence Microscopy

Specimen Preparation. Cells were rinsed with Pipes wash buffer (PWB; 100 mM Pipes, 1 mM EGTA, 1 mM MgSO$_4$, pH 7.2); fixed in fixation buffer (3% formaldehyde freshly prepared from paraformaldehyde in PWB) for 60 min; permeabilized with 0.01% Triton X-100 in PWB (three changes, 5 min each); washed with PWB; rinsed with deionized water; postfixed with methanol at −20°C (5 min); extracted with acetone at −20°C (5 min); and air dried. Before the methanol step all solutions were at room temperature.

Antibody Labeling. After air drying, coverslips were immediately rehydrated with PBS; blocked to eliminate nonspecific binding of antibodies in blocking buffer (5% FBS, 5% glycerin, 0.04% azide in PBS) for 1 h at 37°C; incubated in primary rabbit antibodies (1:500 dilution of anticentrin immune or preimmune serum) overnight at 37°C; washed with PBS; incubated in anti-rabbit rhodamine-conjugated secondary antibody (1:1,000 dilution; CooperBiomedical, Inc., Malvern, PA) for 4 h at 37°C; washed with PBS; rinsed with deionized water to remove salts; and mounted with Elvanol mountant (Rodriquez and Deinhardt, 1960) containing 0.06 g/ml 1,4-diazabicyclo-(2,2,2)-octane (Sigma Chemical Co., St. Louis, MO) to reduce fading of fluorescence.

Cells destined for double labeling were prepared as described above and carried through the anticentrin labeling step. These samples were then washed with PBS; incubated in a 1:20 dilution of mouse monoclonal anti-α-tubulin (this culture supernate was a generous gift of Dr. B. Huang, Research Institute of Scripps Clinic, La Jolla, CA) for 4 h at 37°C; washed with PBS; incubated in secondary antibodies (goat anti-mouse fluorescein-conjugated IgG and goat anti-rabbit rhodamine-conjugated IgG [1:1,000 dilution of each]; CooperBiomedical, Inc.) for 4 h at 37°C; washed with PBS; and mounted.

To reduce nonspecific binding, the secondary antibodies were preabsorbed and crossabsorbed against PtK$_2$ cells that were prepared as described above. Cells were rehydrated, blocked, and incubated overnight in secondary antibodies at 37°C. The antibody supernates were then collected and stored at 0-4°C until use. Just before use, the supernates were centrifuged [15,000 g, 5 min). All antibodies were diluted in PBS.

Photography. Micrographs were taken on a Nikon Optiphot microscope (Nikon Inc., Instrument Div., Garden City, NY) equipped with epifluorescence illumination using a 40× or 100× oil immersion objective. Images were recorded on HyperTech film (Microfluor, Ltd., Stony Brook, NY) and developed with D-19 for 4 min at 68°C.

Electron Microscopy

Fixation of PtK$_2$ cells for electron microscopy was carried out according to the procedure of McDonald (1984). Cells grown on sterile carbon-coated glass coverslips were rinsed with 50 mM cacodylate buffer, pH 7.4, and fixed in 2% glutaraldehyde buffered with cacodylate for 1 h at room temperature. After a buffer wash, the samples were postfixed with 0.5% osmium tetroxide and 0.8% K$_3$Fe(CN)$_6$ in cacodylate buffer for 15 min on ice. Samples were washed with buffer, mordanted with 0.15% tannic acid in cacodylate buffer for 1 min, washed with deionized water, and stained with 2% aqueous uranyl acetate for 1 h at room temperature. After washing with deionized water, the samples were dehydrated through an ethanol series, cleared with propylene oxide, and embedded in Poly/Bed-812. Blocks were polymerized at 60°C for 48 h. Silver-gold interference sections were cut using an ultramicrotome (Reichert Scientific Instruments, Buffalo, NY) and a diamond knife (Diatome-US Co., Fort Washington, PA), collected on Formvar-coated copper grids, poststained at room temperature with 2% aqueous uranyl acetate (15 min), and treated with Reynold's lead citrate for 15 min. Sections were observed and photographed on an electron microscope (model 1200; JEOL USA, Electron Optics Div., Peabody, MA).

Immunogold Labeling for Electron Microscopy

Specimen Preparation. Cells were grown as described under Electron Mi-

croscopy, rinsed once with PWB, and fixed with 3% formaldehyde in PWB for 10 min at room temperature. Cells were permeabilized with 0.5% Triton X-100 for 10 min at room temperature and washed with PBS.

Antibody Labeling. Cells were immediately blocked in blocking buffer for 1 h at 37°C and incubated in primary rabbit antibodies (1:100 dilution of anticentrin immune or preimmune serum) for 1 h at 37°C. The cells were washed with PBS, incubated in 5-nm colloidal gold-conjugated secondary antibodies (1:20 dilution; Janssen Pharmaceutica, Beerse, Belgium) for 3 h at 37°C, washed again with PBS, and processed as described under Electron Microscopy.

Results

Ultrastructural Characteristics of Pericentriolar Material

The cell cycle is intimately coordinated with the centrosome cycle in cultured mammalian cells (Robbins et al., 1968; Stubblefield, 1968; Brinkley and Stubblefield, 1970; Rattner and Phillips, 1973; Rattner and Berns, 1976; Jensen et al., 1979; Rieder et al., 1979; Tucker et al., 1979; Kuriyama and Borisy, 1981*b*; Rieder and Borisy, 1982; Vorobjev and Chentsov, 1982; Kuriyama et al., 1986). It is thus possible to determine the phase of the cell cycle for a particular cell by examining ultrastructural features of the centrosome. Electron micrographs from two separate PtK$_2$ cells in G$_1$ phase of the cell cycle are shown in Fig. 1, *A*, *B* (nonserial sections from the same cell), and *C*, respectively. The oldest centriole (mother) characteristically displays a primary cilium and various centriolar appendages; i.e., alar appendages (transition fibers), basal feet, and a striated root. The daughter centriole of the duplex is typically positioned at a nearly orthogonal angle relative to the mother centriole and does not bear any well formed appendages. Other components of PCM such as pericentriolar satellites and pericentriolar matrix are also illustrated.

Striated roots of PtK$_2$ cells are composed of axially arranged filaments that have a diameter of 7-11 nm (Figs. 1 and 3). The cross-striations of this organelle are approximately 25-nm wide, have a period of 62 nm, and often consist of an electron-lucent central region bordered by electron-opaque regions (Fig. 1 *A*). At their proximal centriole-associated end, the filaments splay and integrate the root with basal feet and pericentriolar matrix. Distally, the root attaches to profiles of smooth membrane. In light of the association of the striated root with centrioles, we consider this organelle a filamentous elaboration of PCM.

Basal feet are conical projections that attach to the centriole wall at their widest end (Figs. 1, *A* and *C*, and 2 *A*). In appropriate sections they appear striated, having alternating light and dark bands that are variable in number, periodicity, and width. An electron-opaque cap is characteristic of their tapered end (Fig. 1 *C*). Numerous microtubules attach to these caps, identifying them as MTOCs. Examination of basal feet, at high magnification, reveals that they are composed of filaments (Fig. 2 *A*). These filaments fall into two size classes; filaments having a diameter of 3-8 and 7-11 nm are distinguishable. Thus, basal feet are composite structures of three distinct filament classes (3-8- and 7-11-nm-diam filaments, and cytoplasmic microtubules); they represent another filamentous elaboration of PCM.

Pericentriolar satellites are irregularly shaped, filamentous, electron-opaque bodies that range in size from 35 to

120 nm (Fig. 2 *B*). They are not membrane delimited and are indirectly connected to centrioles through the pericentriolar matrix. Pericentriolar satellites are similar to basal feet, in that they are composed of and interconnected by 3-8-nm-diam filaments (Figs. 2 *B* and 3). It is important to realize that satellites seen in one thin section are connected to satellites in adjacent thin sections. Pericentriolar satellites are a third elaboration of PCM.

Basal feet and pericentriolar satellites are, in part, composed of 3-8-nm-diam filaments. These filaments are distinct in diameter from the cell's microfilaments (5-10 nm), intermediate filaments (8-13 nm), microtubules (22-29 nm), and striated root filaments (7-11 nm) (Fig. 3). Basal feet and pericentriolar satellites are thus constituents of a filamentous three-dimensional cytoskeletal lattice, which is an integral component of the centrosome.

Identification of a Centrosome-associated Protein in PtK$_2$ Cells

A rabbit antiserum produced against electrophoretically purified centrin has been used in this study to identify an immunologically related protein. Immunoprecipitation of [^{35}S]-methionine- and [^{35}S]cysteine-labeled proteins from PtK$_2$ cells with anticentrin immune serum (lane *A*), preimmune serum (lane *B*), and protein A-Sepharose alone (lane *C*) is illustrated in Fig. 4. Lane *C* shows that protein A-Sepharose nonspecifically precipitates the band with an M_r greater than 200,000. Comparison of *A*-*C* indicates that immune serum specifically immunoprecipitates a protein with an M_r of 165,000. The results suggest that an antigenic epitope common to centrin is carried by this 165,000-M_r protein.

Indirect Immunofluorescent Localization of the 165,000-M$_r$ Protein

Immunofluorescence microscopy of interphase PtK$_2$ cells, labeled by the indirect method with anticentrin antisera, show labeling of a juxtanuclear region within the cytoplasm that is suggestive of the cell's major MTOC, the centrosome (Fig. 5 *A*). Control cells labeled with preimmune serum (Fig. 5 *B*) demonstrate no specific labeling of this region. At higher magnification, the fluorescent pattern consists of a constellation of spots or satellites arranged around one point of origin (Fig. 5 *C*). The satellites closest to the origin are tightly packed. Their proximity to each other and three-dimensional organization produces a brightly fluorescent sphere. We have confirmed the centrosomal location of the 165,000-M_r protein in interphase PtK$_2$ cells by double labeling with antitubulin and anticentrin antibodies (Fig. 6). The anticentrin labeling pattern is organized around the point of origin of the cell's microtubule array thereby identifying this region as the centrosome. The results indicate that the 165,000-M_r protein is a novel centrosome-associated component of PtK$_2$ cells.

Ultrastructural Localization of the 165,000-M$_r$ Protein

Control cells reacted with preimmune serum show background levels of gold label (Fig. 7, *A* and *B*). Sections through both mother and daughter centrioles of a cell in G$_1$ phase of the cell cycle are shown.
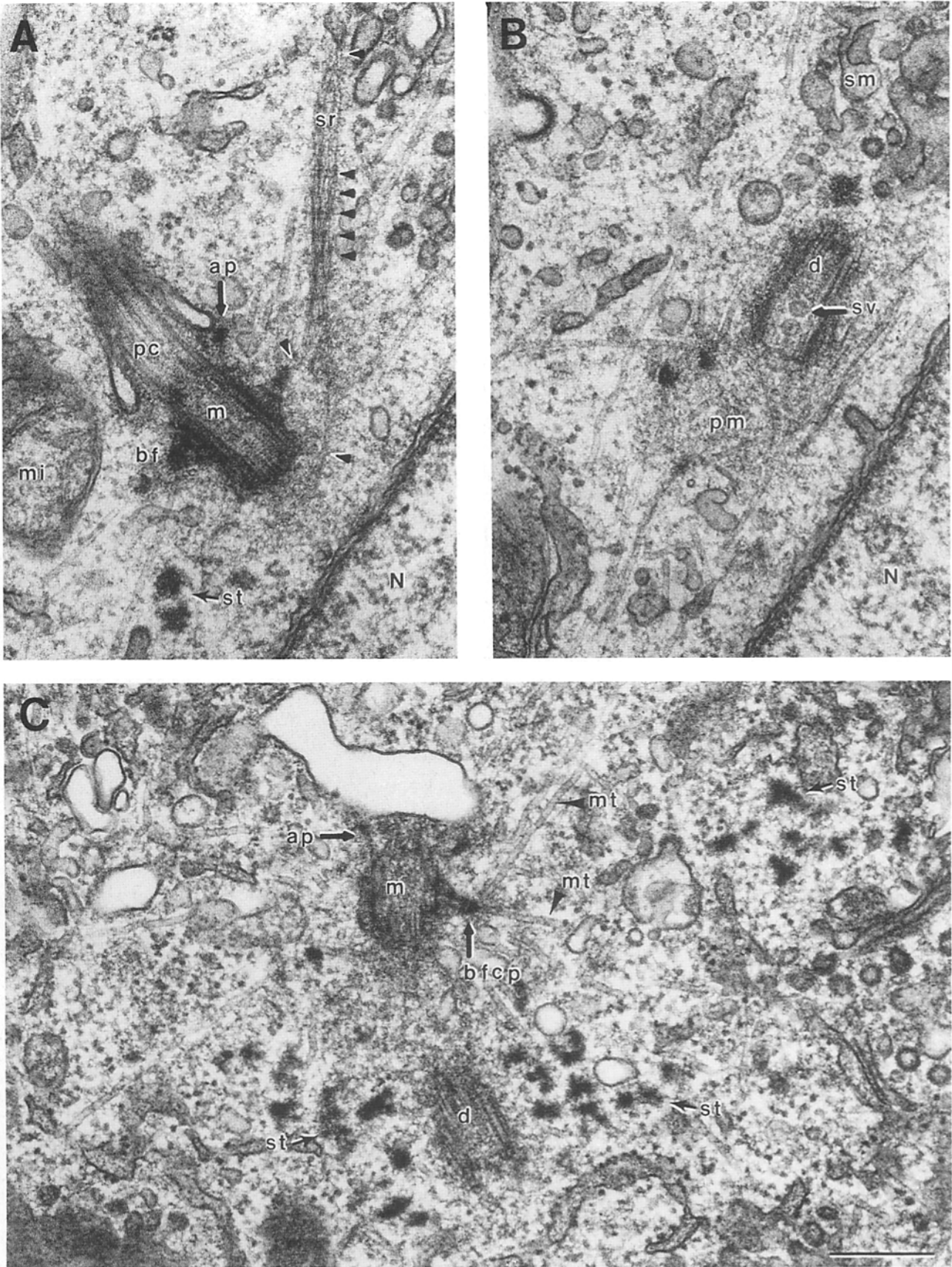
Figure 1. Ultrastructural features of the centrosome and PCM. Shown are sections from two separate cells in G_1 phase of the cell cycle (*A–C*; *A* and *B* are nonserial sections from the same cell). Constituents of PCM shown are alar appendages (*ap*), basal feet (*bf*), a striated root (*sr*), pericentriolar matrix (*pm*), and pericentriolar satellites (*st*). Notice the cross-striations (*black arrowheads*) of the striated root
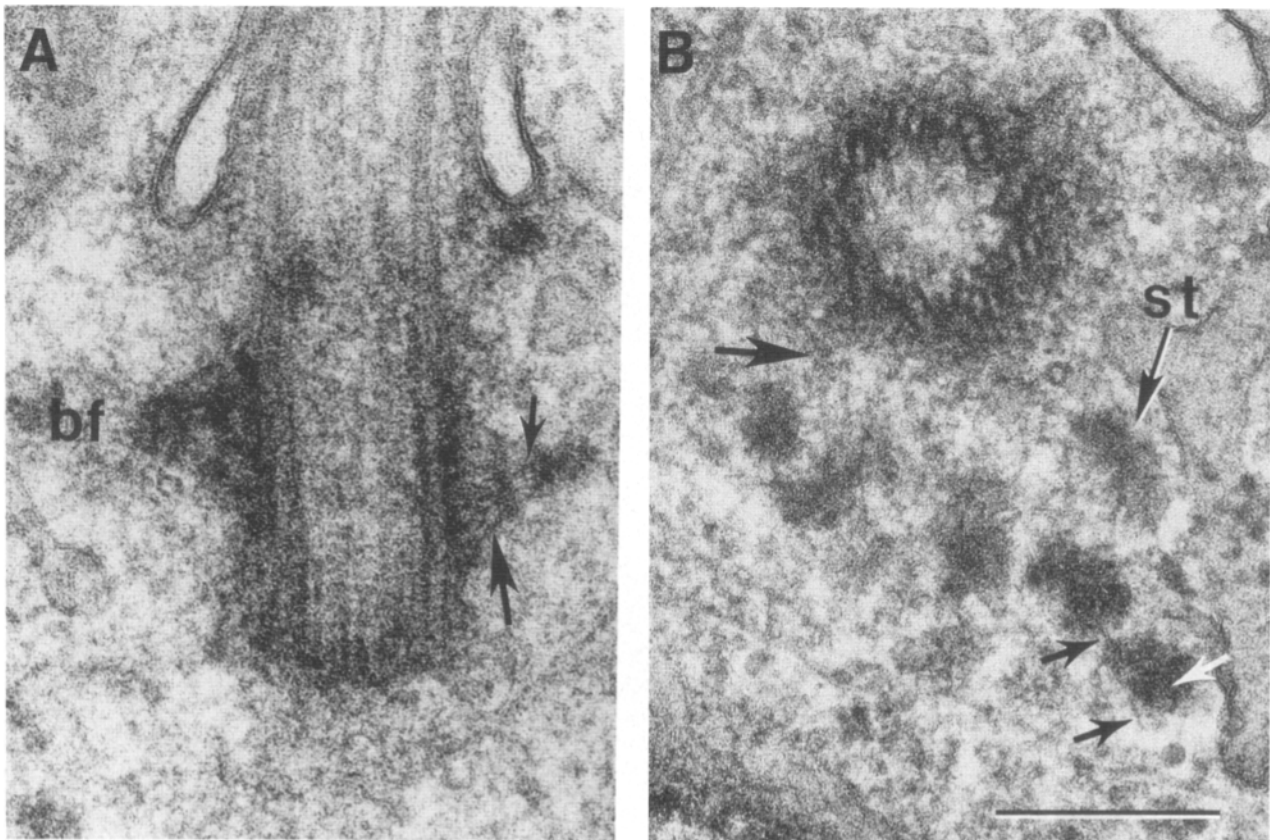
Figure 2. Ultrastructural characteristics of basal feet and pericentriolar satellites. (*A*) This is a higher magnification of the mother centriole shown in Fig. 1 *A*. Basal feet (*bf*) have a striated morphology and are composed of filaments that have diameters of 3–8 (*small arrow*) and 7–11 nm (*large arrow*). (*B*) Pericentriolar satellites are indirectly connected to centrioles through the pericentriolar matrix (*large arrow*) and are composed of and interconnected by 3–8-nm-diam filaments (*small arrows*). Bar, 0.25 μm.

Immunolocalization of the 165,000-M_r protein at ultra-structural resolution with anticentrin immune serum and secondary anti–rabbit IgG conjugated to 5-nm colloidal gold is illustrated in Fig. 7, *C–H*. Fig. 7 *C* shows several labeled pericentriolar satellites in the vicinity of a G_1 duplex. Fig. 7 *D* illustrates another G_1 duplex; pericentriolar satellites, a basal foot, and material adherent to the centriole wall are labeled. In Fig. 7 *E*, several pericentriolar satellites and the pericentriolar matrix material attaching them to the daughter centriole of a G_1 duplex are labeled. Fig. 7, *F–H*, shows serial sections from a cell in G_2 phase of the cell cycle. Two unlabeled striated roots are seen; each root is associated with the older centriole of each duplex. Also seen is a cluster of labeled pericentriolar satellites; these are connected to a daughter centriole by labeled pericentriolar matrix material. The micrographs also demonstrate that gold label seen in one thin section may be associated with pericentriolar satellites in an adjacent section; this is a consequence of the preembedding labeling technique used here. Finally, note that the pericentriolar matrix material (intercentriolar matrix) that lies between the centrioles is unlabeled.

The immunogold localization of the 165,000-M_r protein to pericentriolar satellites, basal feet, and a component of pericentriolar matrix demonstrates that these elements constitute the centrosomal constellation seen by immunofluorescence microscopy. Standard transmission electron microscopy has demonstrated that basal feet and pericentriolar satellites are, in part, composed of 3–8-nm-diam filaments. Taken together, these observations suggest that the 3–8-nm-diam filaments common to basal feet and pericentriolar satellites may, in part, be composed of the 165,000-M_r protein identified in this study. We conclude that the anticentrin antisera used in this study identify a novel pericentriolar cytoskeletal filament system within PtK₂ cells.

Discussion

The 65,000-M_r Protein Is Immunologically Related to Centrin

Antibodies raised against centrin (Salisbury et al., 1984) have been used here to identify a mammalian protein with an M_r of 165,000 in PtK₂ cells. Our observations do not pre-

and its association with a basal foot, profiles of smooth membrane, and pericentriolar matrix (*black and white arrowheads*). Microtubules are also seen to focus at basal foot caps (*bfcp*). *m*, mother centriole; *d*, daughter centriole; *pc*, primary cilium; *N*, nucleus; *mt*, microtubules; *sm*, smooth membrane tubules; *sv*, smooth membrane vesicles; *mi*, mitochondria. Bar, 0.25 μm.
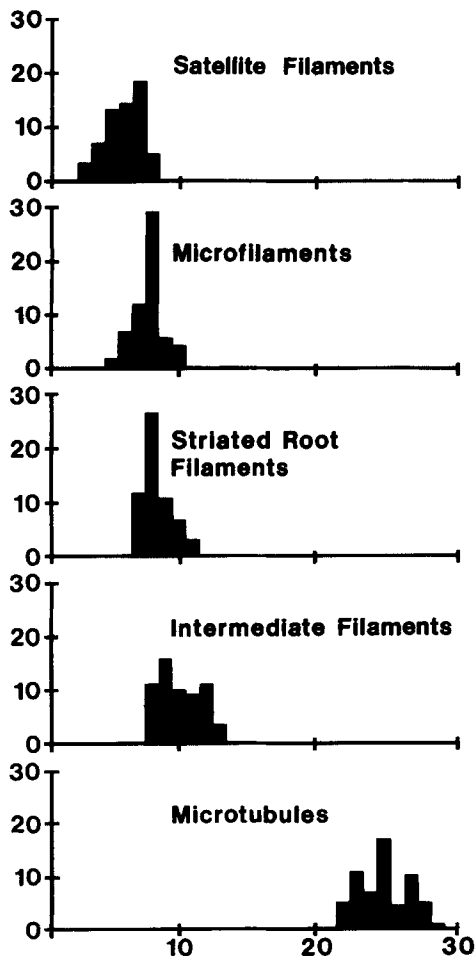
Figure 3. Histograms of filament diameters for microtubules, intermediate filaments, microfilaments, striated roots, and satellite filaments. The mean filament diameters are 25 nm (microtubules), 10 nm (intermediate filaments), 8 nm (microfilaments), 8 nm (striated root filaments), and 6 nm (satellite filaments).

Figure 4. Identification of the 165,000-M_r protein. Autoradiograms of immunoprecipitates after [^{35}S]methionine and [^{35}S]cysteine labeling of whole cell PtK$_2$ with (*A*) anticentrin immune serum, (*B*) preimmune serum, and (*C*) protein A–Sepharose. Molecular mass markers (in kilodaltons) indicated at the left are, from top to bottom, 205,000 (myosin); 116,000 (β-galactosidase); 97,400 (phosphorylase B); 66,000 (BSA); 45,000 (albumin, egg); 29,000 (carbonic anhydrase); 24,000 (trypsinogen); and 18,400 (β-lactoglobulin).

clude the possibility that PtK$_2$ cells contain a low amount of the 20,000-M_r centrin molecule, which is not detectable by our assays. We also acknowledge that the 165,000-M_r protein may be a minor protein contained in our algal centrin preparations. However, we believe this to be unlikely as our antisera were raised against electrophoretically purified centrin, and affinity-purified anticentrin antibodies demonstrate identical immunolocalization patterns as whole immune serum in both algae and PtK$_2$ cells (Baron, A. T., and J. L. Salisbury, unpublished observations). At this time, we cannot reconcile the distinct molecular masses for centrin and the 165,000-M_r protein although several mechanisms to account for these observations can be postulated. These mechanisms are gene duplication and fusion, gene fusion with other genes, and alternate splicing and/or developmental regulation of alternate forms. Discriminating among these possibilities will require dissection of the molecular and genetic basis for these proteins. Regardless of the different molecular masses of centrin and the 165,000-M_r protein of PtK$_2$ cells, anticentrin antibodies demonstrate that these divergent proteins share a conserved epitope(s).

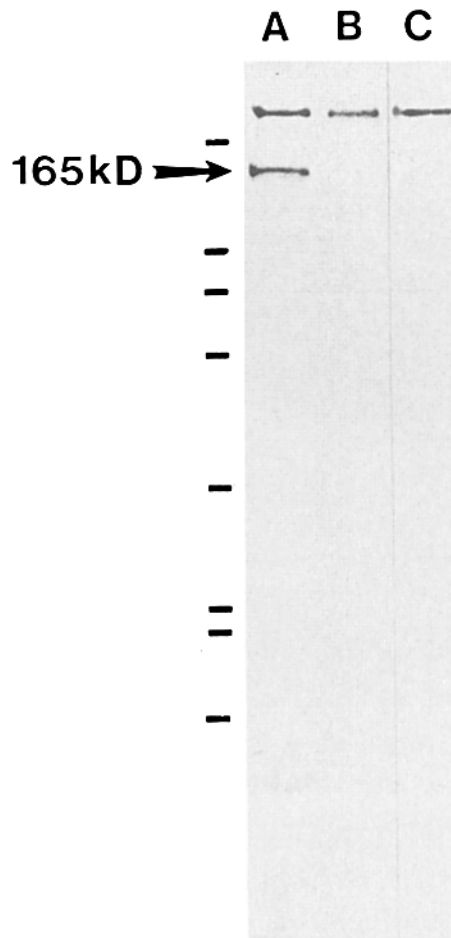Recent molecular cloning of the centrin gene from the alga

Chlamydomonas indicates that centrin shares sequence homology (50% identity) with the CDC31 gene product of *Saccharomyces cerevisiae* (Huang et al., 1988). Cells carrying temperature-sensitive alleles of the CDC31 gene are defective in spindle pole body duplication; the consequence of this defect is cell cycle arrest (Byers, 1981). The spindle pole body of yeast cells represents the major MTOC of these cells, and is therefore homologous to the mammalian centrosome and algal flagellar apparatus. The relationship of centrin, the 165,000-M_r protein of PtK$_2$ cells, and the CDC31 gene product is of interest in light of the latter's importance in cell cycle progression. The association of these immunologic and sequence-related proteins to MTOCs of such divergent phylogenies support the position that a functional attribute(s) indispensible for MTOC function during cell division has been evolutionarily conserved.

Basal Feet, Pericentriolar Satellites, and Pericentriolar Matrix: Immunologic and Structural Relatives of Centrin-based Organelles

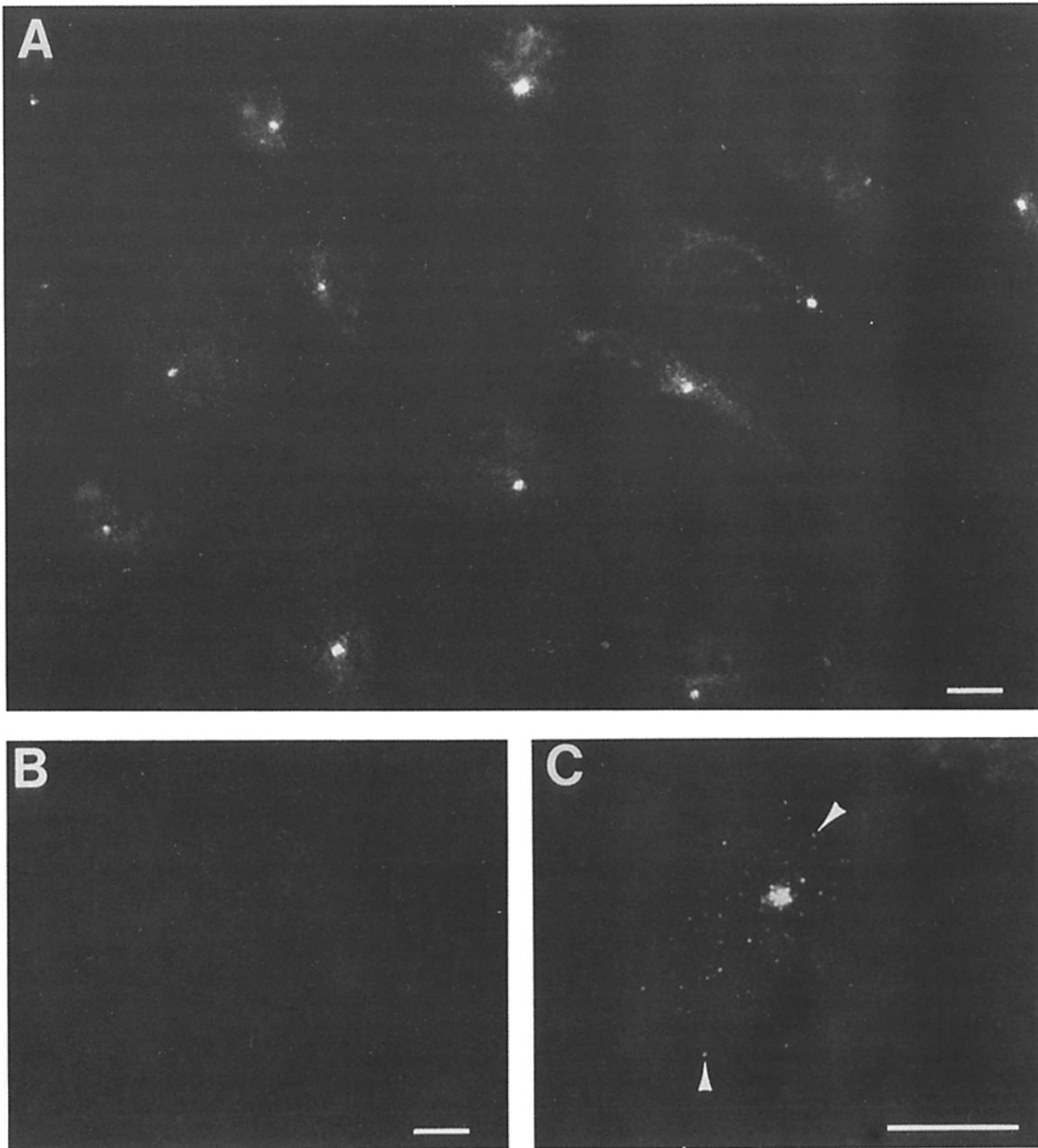This study demonstrates that pericentriolar satellites, peri-

Figure 5. Immunofluorescence localization of the 165,000-M_r protein. Low magnification micrographs of interphase PtK$_2$ cells reacted with (*A* and *C*) anticentrin immune serum and (*B*) preimmune serum are shown. A juxtanuclear region within the cytoplasm that is suggestive of the centrosome labels with immune serum only. (*C*) Higher magnification of an individual cell reveals that the labeling pattern consists of a constellation of spots or satellites (*arrowheads*) arranged around a brightly fluorescent sphere of superimposed satellites. Bars, 10 μm.

centriolar matrix, and basal feet of PtK$_2$ cells share a common immunologic epitope(s) with centrin-based organelles. In addition, these components of PCM also share structural features with centrin-based fiber systems of algal flagellar apparatus.

Immunocytochemical studies have shown that centrin is a component of the nucleus–basal body connectors and distal fibers of *Chlamydomonas reinhardtii* and *Spermatozopsis similis*, and the SFRs of *Tetraselmis striata* (Salisbury et al., 1984, 1986, 1987; Wright et al., 1985; McFadden et al.,

1987). Ultrastructural examination has revealed that SFRs, nucleus–basal body connectors, distal fibers, pericentriolar satellites, and basal feet consist of 3–8-nm-diam filaments (Salisbury, 1983, 1987; Wright et al., 1985; this study). The striated appearance of PtK$_2$ basal feet with respect to variable periodicity and band width is reminiscent of the striation patterns common to SFRs and distal fibers. In addition, pericentriolar satellites are similar to the satellites that form the electron-opaque cross-striations of SFRs during calcium-induced contraction. During contraction the filaments of
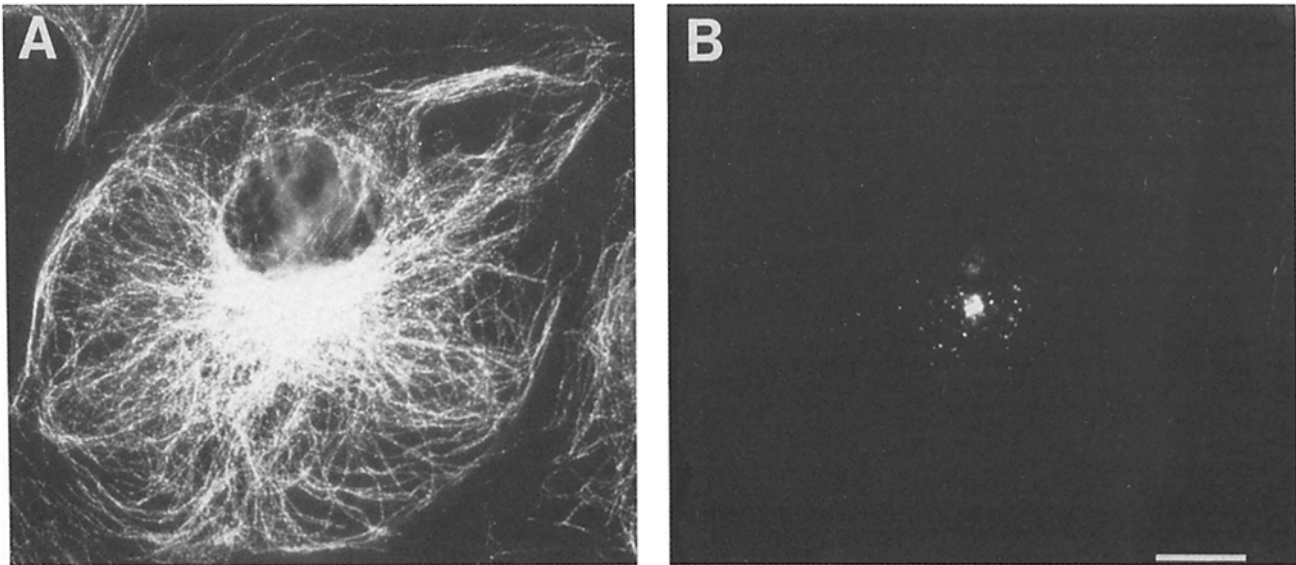
Figure 6. Localization of tubulin and the 165,000-M_r protein. An interphase PtK$_2$ cell double labeled with (A) antitubulin and (B) anticentrin antibodies is shown. The 165,000-M_r protein localizes to the centrosome. Bar, 10 μm.

SFRs twist and supercoil upon themselves to form electron-opaque satellites (Salisbury, 1983); the electron-opaque cross-striations of SFRs thus represent supercoiled filaments. Taken together, these observations suggest that pericentriolar satellites of interphase PtK$_2$ cells, like the satellites of SFRs, are supercoiled filaments.

Previous studies have demonstrated that SFRs of *Tetraselmis* are calcium-modulated contractile organelles, which contract under conditions of high calcium; cycles of contraction and extension are possible when ATP is supplied (Salisbury and Floyd, 1978; Salisbury, 1983). Similar observations have been made in *Chlamydomonas* with regard to the nucleus–basal body connector (Wright et al., 1985; Salisbury et al., 1987). McFadden et al. (1987) have recently shown that the distal fiber of *Spermatozopsis* is a calcium-modulated contractile organelle responsible for basal body reorientation during the photophobic response in flagellated green algae. Experiments examining the calcium sensitivity of pericentriolar satellites of interphase PtK$_2$ cells indicate that high intracellular calcium levels favor their localized appearance in the vicinity of the centrioles whereas low intracellular calcium levels favor their dispersion and disappearance (Baron, A. T., and J. L. Salisbury, unpublished observations). The immunologic and structural relatedness

of the pericentriolar lattice of mammalian centrosomes with centrin-based organelles of algal flagellar apparatus give credence to the possibility that a calcium-modulated function may also have been evolutionarily conserved. The pericentriolar lattice of PtK$_2$ cells may represent a calcium-modulated contractile organelle. The behavior of the pericentriolar lattice during repositioning and/or reorienting the centrosome during directional cell migration (Albrecht-Beuhler, 1977; Gotlieb et al., 1981; Nemere et al., 1985) and mitosis (Rattner and Berns, 1976), and chromosome movement (Cande, 1982; Pickett-Heaps et al., 1984) are currently being investigated in this regard.

References

Albrecht-Buehler, G. 1977. Phagokinetic tracks of 3T3 cells: parallels between the orientation of track segments and of cellular structures which contain actin or tubulin. *Cell.* 12:333–339.

Figure 7. Immunolocalization of the 165,000-M_r protein at ultrastructural resolution. (A and B) Control cells, reacted with preimmune serum, show background levels of gold label. Shown are sections through both mother (m) and daughter (d) centrioles of a cell in G$_1$ phase of the cell cycle. (C–H) Cells reacted with immune serum are shown. (C) Several labeled pericentriolar satellites (st) in the vicinity of a G$_1$ duplex are shown. (D) In another G$_1$ cell, pericentriolar satellites, a basal foot (bf), and the material adherent to the centriole wall (wl) are labeled. (E) Labeled pericentriolar satellites and pericentriolar matrix material attached to a daughter centriole of a G$_1$ duplex are shown. (F–H) Serial sections from a cell in G$_2$ phase of the cell cycle are shown. Two unlabeled striated roots (sr) are seen associated with the grandmother (gm) and mother centrioles. A daughter centriole is also seen. A cluster of labeled pericentriolar satellites are connected to the daughter centriole by labeled pericentriolar matrix material (arrowheads). These micrographs also demonstrate that gold label seen in one thin section may be associated with pericentriolar satellites in an adjacent section (circled satellites and gold label), and that the pericentriolar matrix material (pm) that lies between the centrioles is unlabeled. N, nucleus; mi, mitochondria; if, intermediate filaments; ct, outer cell cortex. Bar, 0.25 μm.

2676
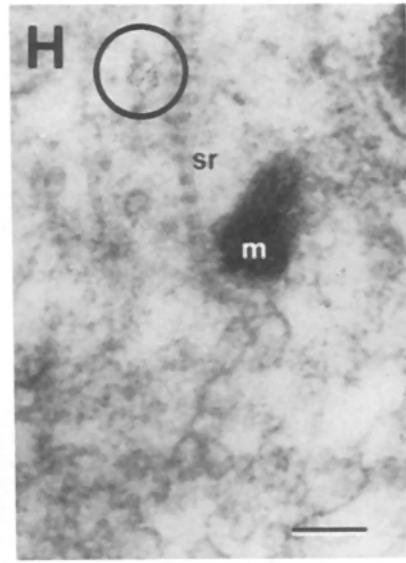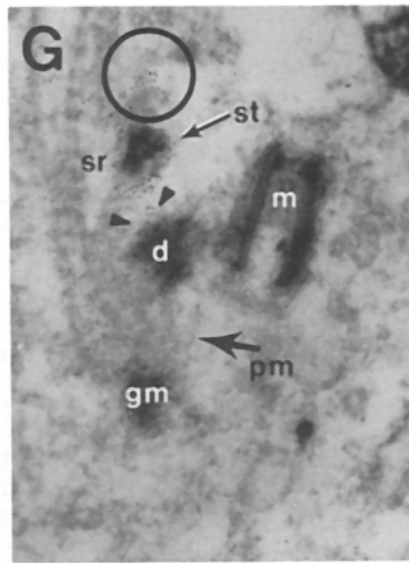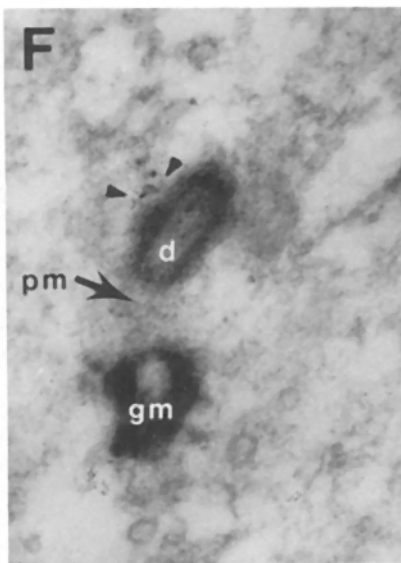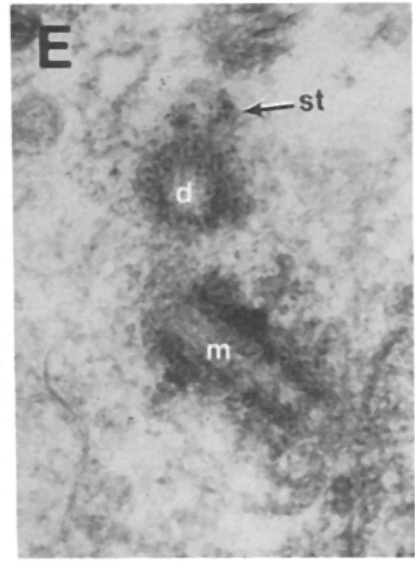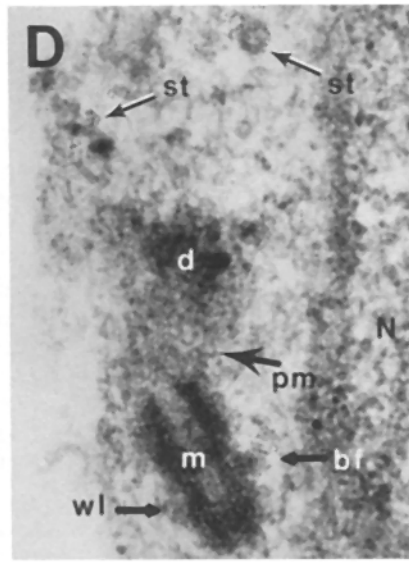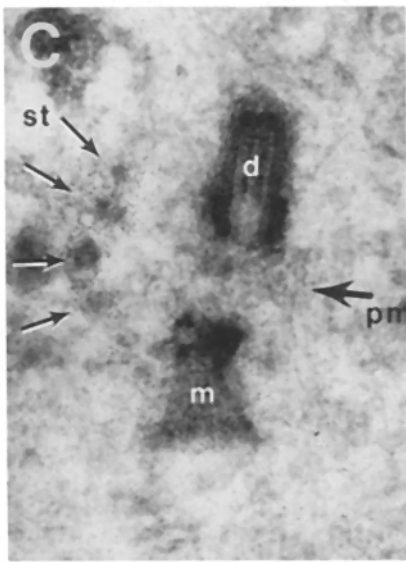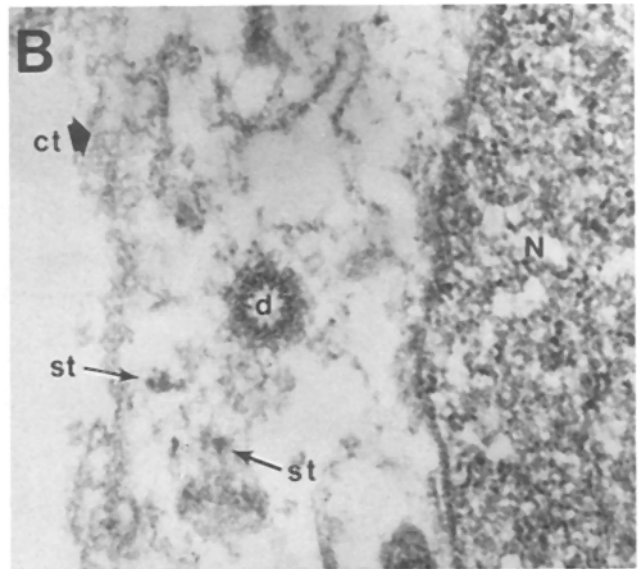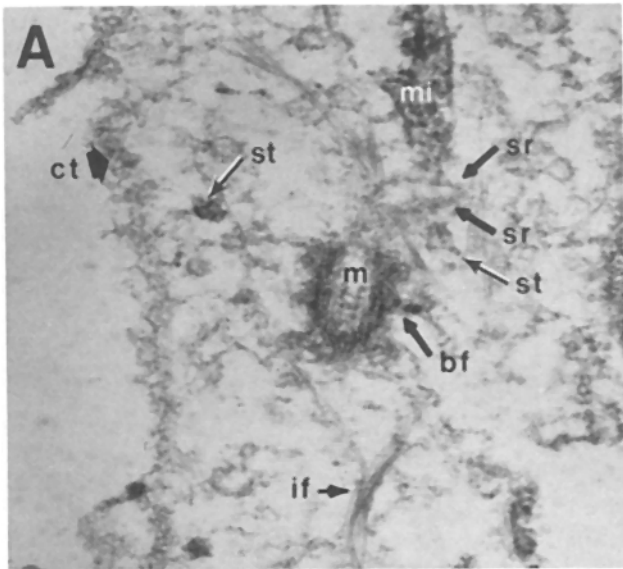
Berns, M. W., and S. M. Richardson. 1977. Continuation of mitosis after selective laser microbeam destruction of the centriolar region. *J. Cell Biol.* 75: 977-982.

Berns, M. W., J. B. Rattner, and S. Brenner. 1977. The role of the centriolar region in animal cell mitosis: a lazer microbeam study. *J. Cell Biol.* 72: 351-367.

Brinkley, B. R. 1985. Microtubule organizing centers. *Annu. Rev. Cell Biol.* 1:145-172.

Brinkley, B. R., and E. Stubblefield. 1970 Ultrastructure and interaction of the kinetochore and centriole in mitosis and meiosis. *Advances in Cell Biology.* 1:119-185.

Byers, B. 1981. Multiple roles of the spindle pole bodies in the life cycle of *Saccharomyces. In* Molecular Genetics in yeast. Vol. 17. D. Von Wettstein, J. Friis, M. Keilland-Brandt, and A. Stenderup, editors. Munksgaard, Copenhagen. 119-131.

Cande, Z. W. 1982. Nucleotide requirements for anaphase chromosome movements in permeabilized mitotic cells: anaphase A but not anaphase B requires ATP. *Cell.* 28:15-22.

Coss, R. A. 1974. Mitosis in *Chlamydomonas reinhardtii.* Basal bodies and the mitotic apparatus. *J. Cell Biol.* 63:325-329.

DeHarven, E. 1968. The centriole and the mitotic spindle. *In* The Nucleus. A. J. Dalton and F. Haquenae, editors. Academic Press Inc., New York. 197-227.

Doonan, J. H., and C. Grief. 1987. Microtubule cycle in *Chlamydomonas reinhardtii*: an immunofluorescence study. *Cell Motil. Cytoskeleton.* 7:381-392.

Gotlieb, A. I., L. M. May, L. Subrahmanyan, and V. I. Kalnins. 1981. Distribution of microtubule organizing centers in migrating sheets of endothelial cells. *J. Cell Biol.* 91:589-594.

Gould, R. R., and G. G. Borisy. 1977. The pericentriolar material in Chinese hamster ovary cells nucleates microtubule formation. *J. Cell Biol.* 73: 601-615.

Huang, B., A. Mengersen, and V. D. Lee. 1988. Molecular cloning of cDNA for caltractin, a basal body-associated Ca^{2+}-binding protein: homology in its protein sequence with calmodulin and the yeast CDC31 gene product. *J. Cell Biol.* 107:133-140.

Jensen, C. G., L. C. W. Jensen, and C. L. Rieder. 1979. The occurrence and structure of primary cilia in a subline of *Potorous tridactylus. Exp. Cell Res.* 123:444-449.

Johnson, U. W., and K. R. Porter. 1968. Fine structure of cell division in *Chlamydomonas reinhardtii. J. Cell Biol.* 38:403-425.

Karsenti, E., and B. Maro. 1986. Centrosomes and the spatial distribution of microtubules in animal cells. *Trends Biochem. Sci.* 11:460-463.

Kuriyama, R., and G. G. Borisy. 1981a. Microtubule-nucleating activity of centrosomes in Chinese hamster ovary cells is independent of the centriole cycle but coupled to the mitotic cycle. *J. Cell Biol.* 91:822-826.

Kuriyama, R., and G. G. Borisy. 1981b. Centriole cycle in Chinese hamster ovary cells as determined by whole-mount electron microscopy. *J. Cell Biol.* 91:814-821.

Kuriyama, R., S. Dasgupta, and G. G. Borisy. 1986. Independence of centriole formation and initiation of DNA synthesis in Chinese hamster ovary cells. *Cell Motil. Cytoskeleton.* 6:355-362.

Laemmli, U. K. 1970. Cleavage of structural proteins during the assembly of the head of bacteriophage T4. *Nature (Lond.).* 227:680-685.

Mazia, D. 1987. The chromosome cycle and the centrosome cycle in the mitotic cycle. *Int. Rev. Cytol.* 100:49-92.

McDonald, K. 1984. Osmium ferricyanide fixation improves microfilament preservation and membrane visualization in a variety of animal cell types. *J. Ultrastruct. Res.* 86:107-118.

McFadden, G. I., D. Schulze, B. Surek, J. L. Salisbury, and M. Melkonian. 1987. Basal body reorientation mediated by a Ca^{2+}-modulated contractile protein. *J. Cell Biol.* 105:903-912.

McIntosh, J. R. 1983. The centrosome as an organizer of the cytoskeleton. *Mod. Cell Biol.* 2:115-142.

McIntosh, J. R. 1987. Progress in research on mitosis. *In* Biomechanics of Cell Division. N. Akkas, editor. Plenum Publishing Corp., New York. 123-143.

Nemere, I., A. Kupfer, and S. J. Singer. 1985. Reorientation of the Golgi ap-

paratus and the microtubule-organizing center inside macrophages subjected to a chemotactic gradient. *Cell Motil. Cytoskeleton.* 5:17-29.

Peterson, S. P., and M. W. Berns. 1980. The centriolar complex. *Int. Rev. Cytol.* 64:81-106.

Pickett-Heaps, J. D. 1969. The evolution of the mitotic apparatus: an attempt at comparative ultrastructural cytology in dividing plant cells. *Cytobios.* 3:257-280.

Pickett-Heaps, J. D., T. Spurch, and D. Tippit. 1984. Chromosome motion and the spindle matrix. *J. Cell Biol.* 99(Suppl.):137s-143s.

Rattner, J. B., and M. B. Berns. 1976. Centriole behavior in early mitosis of rat kangaroo cells (PtK_2). *Chromosoma (Berl.).* 54:387-395.

Rattner, J. B., and S. G. Phillips. 1973. Independence of centriole formation and DNA synthesis. *J. Cell Biol.* 57:359-372.

Rieder, C. L., and G. G. Borisy. 1981. The attachment of kinetochores to the pro-metaphase spindle in PtK_1 cells. Recovery from low temperature treatment. *Chromosoma (Berl.).* 82:693-716.

Rieder, C. L., and G. G. Borisy. 1982. The centrosome cycle in PtK_2 cells: asymmetric distribution and structural changes in the pericentriolar material. *Biol. Cell.* 44:117-132.

Rieder, C. L., C. G. Jensen, and L. C. W. Jensen. 1979. The resorption of primary cilia during mitosis in a vertebrate (PtK_1) cell line. *J. Ultrastruct. Res.* 68:173-185.

Ringo, D. L. 1967. Flagellar motion and fine structure of the flagellar apparatus in *Chlamydomonas. J. Cell Biol.* 33:543-571.

Robbins, E., G. Jentzsch, and A. Micali. 1968. The centriole cycle in synchronized Hela cells. *J. Cell Biol.* 36:329-339.

Rodriquez, J., and F. Deinhardt. 1960. Preparation of a semipermanent mounting medium for fluorescent antibody studies. *Virology.* 12:316-317.

Salisbury, J. L. 1983. Contractile flagellar roots: the role of calcium. *J. Submicrosc. Cytol.* 15:105-110.

Salisbury, J. L. 1988. The lost neuromotor apparatus of *Chlamydomonas*: rediscovered. *J. Protozoology.* 35:574-577.

Salisbury, J. L., and G. L. Floyd. 1978. Calcium-induced contraction of the rhizoplast of a quadriflagellate green alga. *Science (Wash. DC).* 202:975-977.

Salisbury, J. L., A. T. Baron, B. Surek, and M. Melkonian. 1984. Striated flagellar roots: isolation and partial characterization of a calcium-modulated contractile organelle. *J. Cell Biol.* 99:962-970.

Salisbury, J. L., A. T. Baron, D. E. Coling, V. E. Martindale, and M. A. Sanders. 1986. Calcium-modulated contractile proteins associated with the eucaryotic centrosome. *Cell Motil. Cytoskeleton.* 6:193-197.

Salisbury, J. L., M. A. Sanders, and L. Harpst. 1987. Flagellar root contraction and nuclear movement during flagellar regeneration in *Chlamydomonas reinhardtii. J. Cell Biol.* 105:1799-1805.

Schulze, D., H. Robenek, G. I. McFadden, and M. Melkonian. 1987. Immunolocalization of a Ca^{2+}-modulated contractile protein in the flagellar apparatus of green algae: the nucleus-basal body connector. *Eur. J. Cell Biol.* 45:51-61.

Stubblefield, E. 1968. Centriole replication in a mammalian cell. *In* The Proliferation and Spread of Neoplastic Cells. Williams and Wilkins, Baltimore. 175-193.

Telzer, B. R., and J. L. Rosenbaum. 1979. Cell cycle-dependent, in vitro assembly of microtubules onto the pericentriolar material of HeLa cells. *J. Cell Biol.* 81:484-497.

Tilney, L. G., and J. Goddard. 1970. Nucleating sites for the assembly of cytoplasmic microtubules in the ectodermal cells of blastulae of *Arbacia punctulata. J. Cell Biol.* 46:564-575.

Tucker, R. W., A. B. Pardee, and K. Fujiwara. 1979. Centriole ciliation is related to quiescence and DNA synthesis in 3T3 cells. *Cell.* 17:527-535.

Vorobjev, I. A., and Y. S. Chentsov. 1982. Centrioles in the cell cycle. I. Epithelial cells. *J. Cell Biol.* 98:938-949.

Wolfe, J. 1972. Basal body fine structure and chemistry. *Adv. Cell Mol. Biol.* 2:151-192.

Wright, R. L., J. L. Salisbury, and J. W. Jarvik. 1985. A nucleus-basal body connector in *Chlamydomonas reinhardtii* that may function in basal body localization or segregation. *J. Cell Biol.* 101:1903-1912.